

CHAPTER 2

Literature Review

2 LITERATURE REVIEW

2.1 Introduction

This chapter presents a literature review which focuses on two crucial aspects in this work. The first constitutes a review of the various deposition types normally employed in the fabrication of carbon nitride CN_x films. It was from the list of these deposition methods that the deposition employed in this work was chosen. Secondly, a review of the various properties of carbon nitride determined, using the analytical methods employed in this study, is presented. This is an important part of this review since the interpretation of the measurement data are an integral part in the characterization of the films.

2.2 Review on Common Deposition Techniques for Carbon Nitride films

The properties and resulting structure of the carbon nitride films are known to be strongly dependent on precursor materials, deposition types and parameters. Common types of the deposition methods for the fabrication of carbon-based thin films could be divided into two categories which include physical and chemical vapour depositions. Physical methods such as sputtering (direct current, magnetron and radio frequency), pulsed laser ablation and ion-assisted deposition methods use energetic particle bombardment of a suitable target or substrate in a suitable environment to manipulate the resulting films' structural properties and composition (Popov et al. 1999). On the

other hand chemical methods made up of various modifications of chemical vapour deposition (CVD) such as laser CVD, thermal CVD plasma enhanced CVD (PECVD) are based on chemical reaction kinetics (Popov et al. 1999). Since the types of deposition method employed is a crucial determining aspect in the structural formation of these films, it was deemed necessary to give a short review of some of the most common techniques for the deposition of carbon nitride thin films. Here the reviews are based on studies done on carbon based films since the systems setups are identical to those used for carbon nitride films.

2.2.1 Laser Ablation

Pulsed-laser deposition (PLD) is a well-established technique for the synthesis of carbon-based amorphous materials including diamond-like carbon and nitrogenated carbon films (Cappelli et al. ; Riascos et al. 2006). PLD is a technique whereby a pulsed laser beam is focused onto a target material inside a vacuum system. The energy at the focal point is so great that it causes the target material to ablate off, fly across the vacuum chamber, and then stick to a nearby substrate, producing a thin film. The major advantages of PLD are the ability to form hydrogen-free films (Sharma et al. 2000) from congruent evaporation with good crystallinity due to the presence of high-energy evaporants and fast response time (Szörényi and Geretovszky 2004). This allows the technique to form high quality DLC with a high proportion of sp^3 hybridized carbon atoms (Honglertkongsakul et al. 2010). The structural uniformity could be improved by simply changing the orientation of the substrate with respect to the target surface which would decrease the co-deposition of micron and sub-micron particles (Szörényi and Geretovszky 2004). Additionally, with the appropriate monitoring of its deposition

parameters, this technique enables a fair control of nanoparticle size which allows high quality and high purity single walled CNT to be produced (Aïssa et al. 2011).

Figure 2.1 shows several conventional PLD systems made up of a laser source, carbon (graphite) target and biased or non-biased substrate configuration. The laser ablation produce a radiation “plume”, where its dynamics and behaviour strongly affects the deposition process and film properties (Shen et al. 2006). For formation on DLC with a high sp^3 content, the kinetic energies of carbon ions in the plume and substrate temperatures are the main controlling parameters (Honglertkongsakul et al. 2010). The kinetic energies of the species ions are controlled by the energy (wavelength) of the laser radiation source (Cappelli et al. 2011a). Common sources include excimer (XeCl or ArF) and Nd:YAG lasers, which form thin films with smooth surface morphologies.

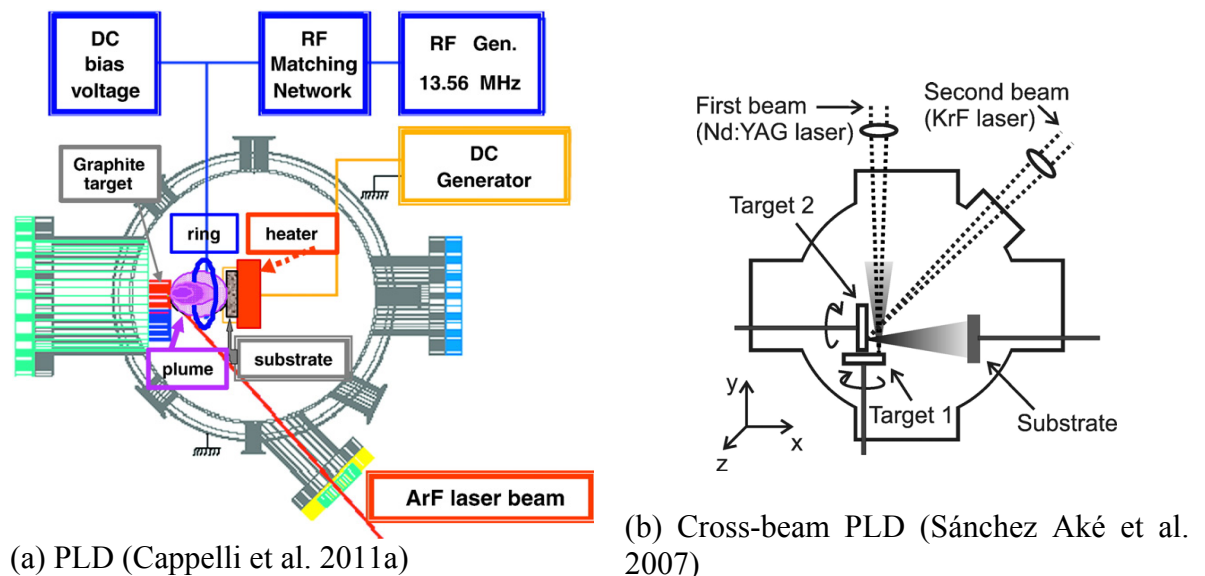


Figure 2.1: Schematic diagrams of various configurations of pulsed laser ablation systems

Hybrid systems such as those shown in Figure 2.2 are usually employed in the formation of nitrogen doped carbon films. The additional glow discharge source allows for the production of a reactive ambient where chemical reactions of the ablated species

with the species in the reactive ambient play a crucial role in film deposition (Shen et al. 2006). The limitation in the widespread usage of PLD is the small area capability, slow deposition rate and high cost.

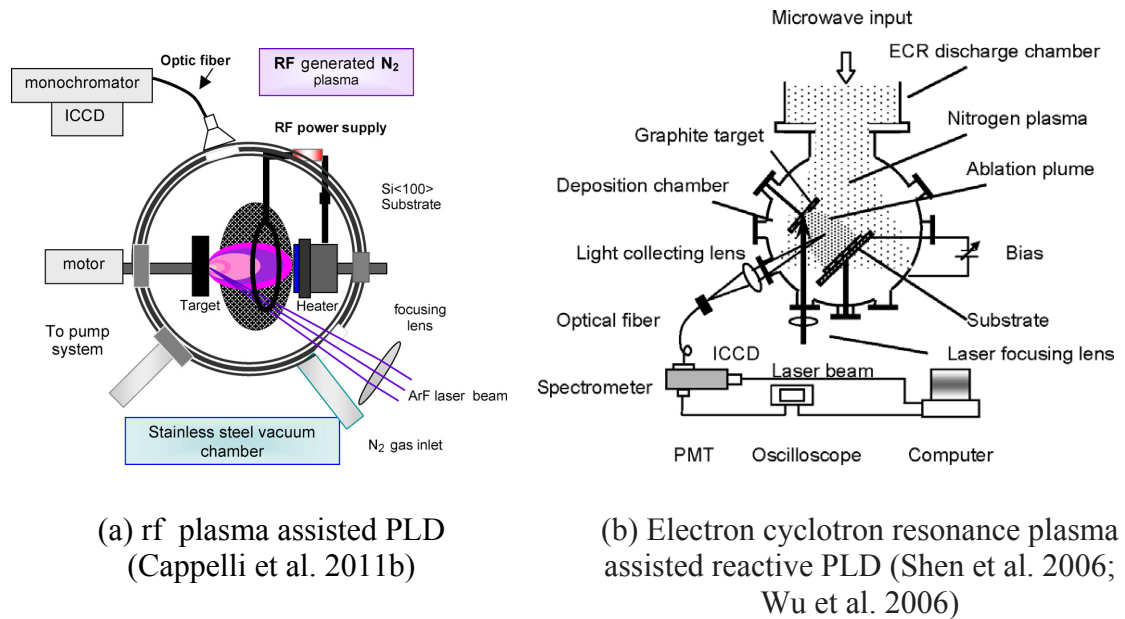


Figure 2.2: Schematic diagrams of two configurations of hybrid pulsed laser ablation systems

2.2.2 Sputtering

Sputtering is said to be the most common industrial process for the deposition of DLC films (Nakazawa et al. 2010). In sputtering technique, a material used as a solid sputtering target is normally placed on an rf or dc powered electrode. Due to bias applied on this electrode, energetic particle generated from an inert gas plasma typically Ar would bombard the target surface. When the bombardment energy is strong enough, atoms from the target could be ejected or sputter out. When these atoms reach a substrate, thin films could be deposited. Sputtering has many advantages such as process simplicity, control and film homogeneity (Alibart et al. ; Myung et al. 2006). This method could also be used to produce hydrogen-free films particularly for DLC

fabrication. This is important since hydrogen-free DLC films show higher thermal stability than their hydrogenated counterparts and also makes sputtering very useful for studies on the effects of the addition of foreign elements or dopants on the film properties. Two of the most common sputtering system configurations including dc magnetron (Fitzgerald et al. 2001; Ujvári et al. 2001) and rf magnetron (Alibart et al. ; I. Banerjee et al. 2010; Du et al. 2007; Lejeune et al. 2004; Nakazawa et al. 2010). However, low deposition rate is the major disadvantage in the deposition of carbon films due to the low sputtering yield of carbon (Myung et al. 2006). For this reason there are a number of modified systems used to resolve this limitation. Examples of these systems are the unbalanced (Wang et al. 2011c) and closed field (Myung et al. 2006; Park et al. 2005) unbalanced magnetron systems, middle frequency magnetron sputtering (Huang et al. 2007b; Zhang et al. 2010a) and ion beam sputtering (Gago et al. 2005; Huang et al. 2003; Lu et al. 1999; Wu et al. 1999; Zhou et al. 2002). Examples of these systems are shown in Figure 2.3.

One of the common features in the sputtering techniques which is similar to other methods, such as plasma enhanced CVD, is the use of positive ion bombardment on the growing film to affect film chemistry and atomic order, from which all other film properties are derived (Kaltofen et al. 1997). This in turn is greatly affected by the substrate temperature and applied power (dc, rf, etc.) values. During the growth process, the applied power affects the flux of neutral particles and ions, and the reactivity of the discharge plasma (Bouchet-Fabre et al. 2008). Other researchers have also intensively studied the effects of substrate biasing which is said to enhance the properties of the films (Li et al. 2002; Wang et al. 2011c; Yasui et al. 2004).

Additionally, sputtering allows the deposition of carbon nitride (Mubumbila et al. 2004; B. Zhang et al. 2010a). In most cases this implies the usage of precursor gas such that the incorporation of these elements may occur through the reactivity within the discharge plasma. Sputtering allows hydrogen-free synthesis of CN_x films which could produce hard film coatings (Ru et al. 2010). Recently, this method has shown to be able to produce graphite-like CN_x films with controllable sp^3 content and low stress level, nanoporous, nanocolumn (Zhang et al. 2010a) and nanostructured films (Banerjee et al. 2010). Apart from the low deposition rate, these sputtering techniques also seem to be limited in term of the flexibility in depositing various structured films especially for tabular nanostructures such as CNTs, nanofibers, etc.

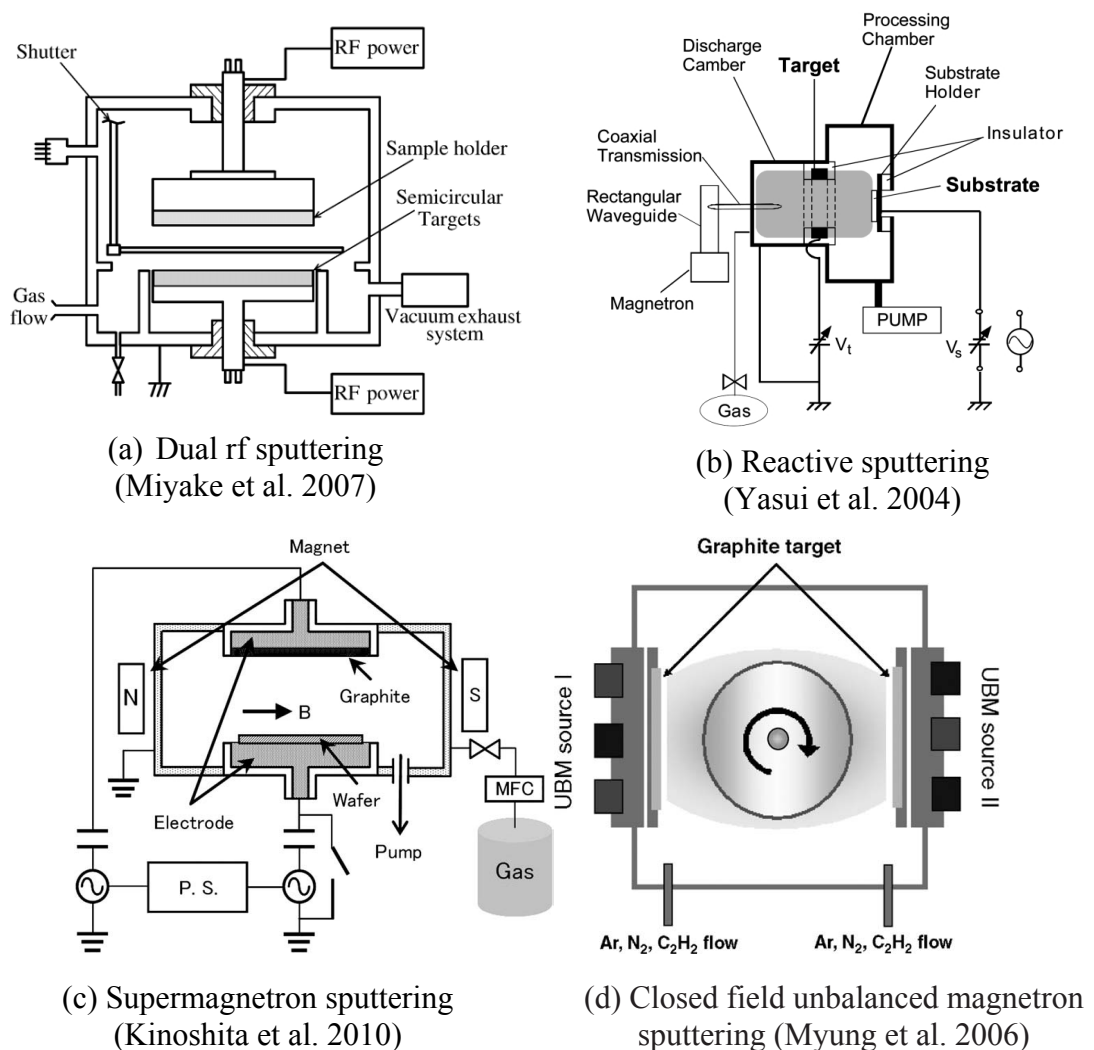


Figure 2.3: Schematic diagrams of different variations of sputtering systems.

2.2.3 *Chemical vapour deposition*

Chemical vapour deposition (CVD) methods are without doubt the most frequently used technique in the deposition of carbon films. This is mainly due to the many simple modifications that can be made to the systems and the control of the film growth that these modifications provide. In a typical CVD process, substrates are exposed to volatile gaseous precursors, which react and/or decompose on the substrate surface and subsequently is deposited in a form of a film. There are a number of methods used to induce the reaction and/or decomposition of these precursors. Two common types include thermal and plasma assisted processes. Thermal methods employing catalytic CVD is the most frequent used method to fabricate CNTs (Sharma and Lakkad 2009) and doping of graphene with N (Imran Jafri et al. 2010). Two typical thermal dissociation techniques for the formation of carbon films include hot-filament (or hot-wire) and thermal CVD.

Popular variations of CVD employing plasma enhanced (or sometimes referred to as plasma assisted) CVD (PECVD) techniques has led to a further increase in the production of various structured films. PECVD promotes good film adhesion even for low substrate temperature (Ni et al. 2008). PECVD techniques are also often employed in the fabrication of nanostructured carbon films. They also allow precise control over these nanofiber or nanofilament length, diameter and positioning (García-Céspedes et al. 2007). Excellent vertically aligned growth of these structures, guided by the direction of the electric field established in the plasma sheath (Bower et al. 2000; Denysenko and Azarenkov 2011) could be fabricated. Moreover through careful manipulation of the deposition parameters, individual freestanding nanostructures could be produced (Le Poche et al. 2007; Weeks et al. 2008; Zhu et al. 2011). Different types of common

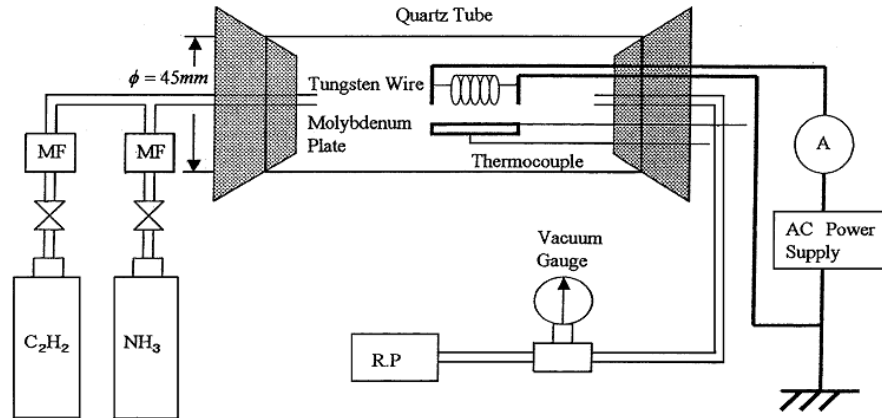
PECVD systems are also discussed in the upcoming sections with regards to the different types of applied power to the plasma.

2.2.3.1 Hot-wire or hot-filament chemical vapour deposition

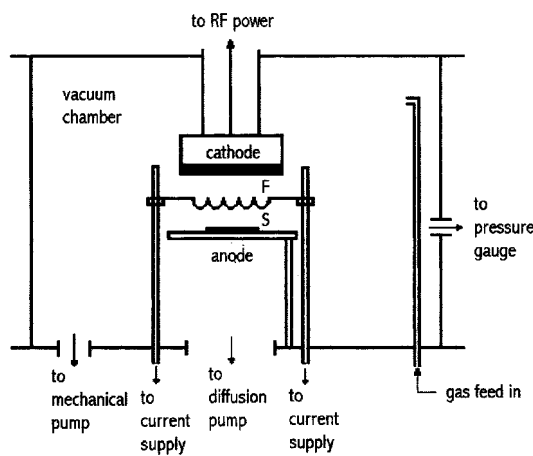
A typical hot-filament (HF)CVD setup employs a metal filament with high melting point (Aono et al. 2008) which dissociated the gases and enables the reaction to occur. The resulting material could reach a substrate to form the film. Examples of HFCVD setups are shown in Figure 2.4. HFCVD has the advantage that the setup can be simple and inexpensive to assemble. It is also one of the promising thermal dissociation techniques for large area thin film deposition (Swain et al. 2009). HFCVD is one of the most common methods used in the deposition of diamond and diamond-like carbon where the hydrocarbon source gas is often used. However this method has the disadvantage that the choice of gas and type of filament are restricted. Some of the problems face by this method are the contamination from filament metals and the tendency of the filament to change into a carbide (Aono et al. 2008). The most common filament used for HFCVD is tungsten (Mitra et al. 2003; Swain et al. 2009; Yokomichi et al. 2001; Zhang et al. 1999a) , though studies show that the use of alternatives such as graphite or amorphous carbon could reduce the problem of contamination considerably (Aono et al. 2008).

The latest work in HFCVD technique show its versatility in the production of carbon nanostructures. These structures include the catalytic-free deposition of carbon nanowalls (Dikonimos et al. 2007) and nanotips (Dang and Wang 2006; Wang and

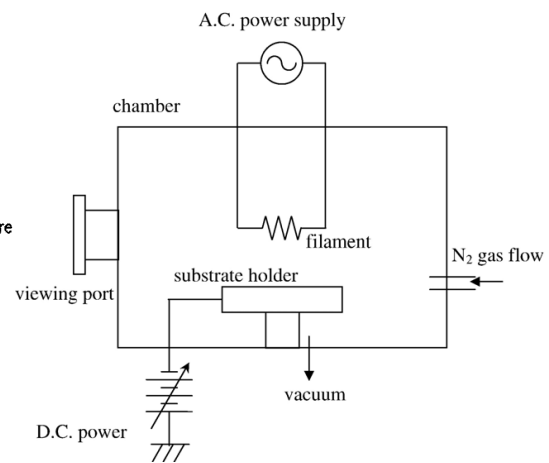
Zhang 2006) and the catalytic deposition of nanocrystalline diamond (Li et al. 2009a), carbon nanotubes (Kim et al.) and carbon nanowalls (Takashi Itoh ; Lisi et al. 2011).



(a) (Yokomichi et al. 2001)



(b) (Jianjun Wang et al. 2000)



(c) HW-rf PECVD
(Aono et al. 2008)

Figure 2.4: Schematic diagrams of two different variations of HFCVD systems (a) and (b) and a HF – rf PECVD hybrid system (c).

For the fabrication of CN_x films, a mixture of a hydrocarbon precursor and nitrogen (Aono et al. 2008) or ammonia (Swain et al. 2009) are often used. This method usually produces hydrogen-free CN_x films, although to produce hydrogenated CN_x films, hydrogen gas could be asserted into the mixture similar to the method employed for hydrogenated carbon films (Shimabukuro et al. 2008). However, due to the high

dissociation energy of N_2 and NH_3 , the nitrogen content in these CN_x films may be relatively low. Indeed, the N content (atm %) in these films has been reported to be a moderate 12 % (Swain et al. 2009). Furthermore the temperature range for these depositions is too high and not suitable for fabrication of electronic devices (Mamalis et al. 2004). These limitations may be the reasons why there are relatively few published reports on CN_x films using this method.

2.2.3.2 Thermal chemical vapour deposition

A typical thermal (T) CVD utilize the heating effect brought by a remote heating source to induce reaction of gaseous precursors. The reactants could be deposited onto a substrate to form the film. Common TCVD setup usually employs a quartz tube inside a furnace which acts as the heating source. Although TCVD is seldom used in the fabrication of amorphous carbon thin films, this technique is one of the most common ways to deposit carbon nanostructured films (Zhao et al. 2011a). However, in most cases the formation of these structures requires the use of metal or alloy catalysis. Examples of TCVD setup as shown in Figure 2.5.

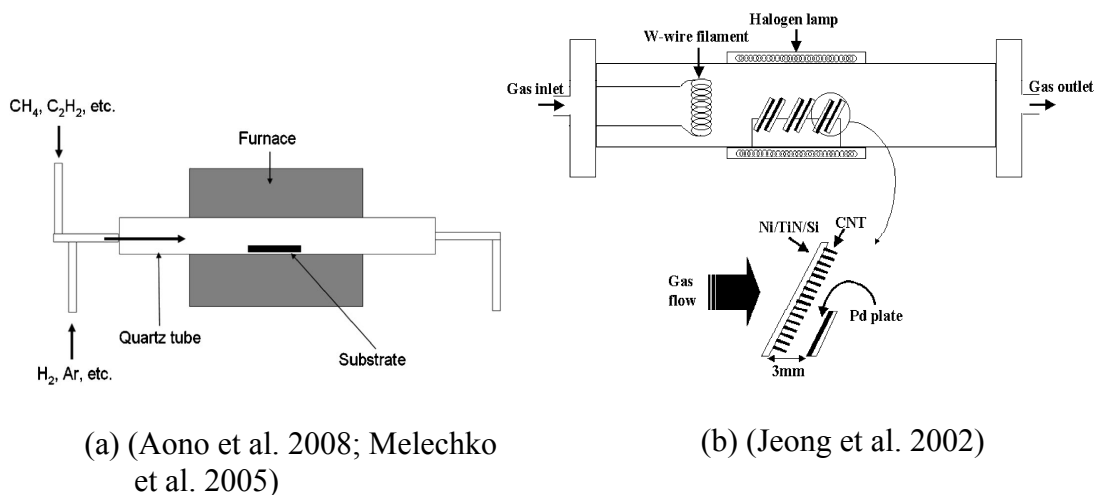


Figure 2.5: Schematic diagrams of two different variations of TCVD systems.

Process temperature for the production of carbon nanostructures typically lie in the range of 400 – 1000 °C (Melechko et al. 2005). A wide variation in structures has been produced by means of catalytic TCVD. These includes carbon nanofibers (Melechko et al. 2005; Sohn et al. 2002), single and multi-walled CNTs (Lee et al. 2008; Liu et al. 2008; Sharma and Lakkad 2009; Suzuki and Hibino; Ting and Lin 2007), and graphene (Zhao et al. 2011a). There are also a number of reports on the formation of various CN_x films. These include CN_x nanostructured thin films (Kurt et al. 2001), hollow vessels (Li et al. 2010) and nitrogen doped CNTs (Maldonado et al. 2006; Xu et al. 2010; Zhao et al. 2011b). Y. Li et al. (Li et al. 2010) and Zhao et al. (Zhong et al. 2010) even claimed of high-N-content CN_x films obtained from TCVD. However, the disadvantage of this method is the lack of control in the alignment of the nanostructures, patterning and control over individual nanostructure growth.

2.2.3.3 Microwave plasma enhanced chemical vapour deposition

In typical microwave plasma enhanced chemical vapour deposition, MWPECVD system, consist of a chamber with a parallel plate electrode configuration. One of the electrode acts as the substrate holder, while the other is connected to a microwave generator. The use of MW is to discharge the gas precursors to produce plasma which enhances the chemical reaction rates of the precursors. The decomposition and reactions in the plasma would induce the formation of species that form the film on substrates. Figure 2.6 shows a number of different setups for, MWPECVD.

MWPECVD is of interest for obtaining crystalline and polycrystalline carbon and carbon nitride films due to the high gas temperature and high dissociation rates that it offers (Kouakou et al. 2008; Uddin et al. 2005). This method is also said to show a superiority in terms of the quality of plasma discharge (Ghimire et al. 2008). Apart from DLC film formation, the versatility in this method is also proven by its capability to form a number of different carbon nanostructured films, such as ultra-nanocrystalline diamond (Zou et al. 2010), carbon nanotubes (Srivastava et al. 2006), nanowalls (Chuang et al. 2006) and nanoropes (Hiramatsu et al. 2003).

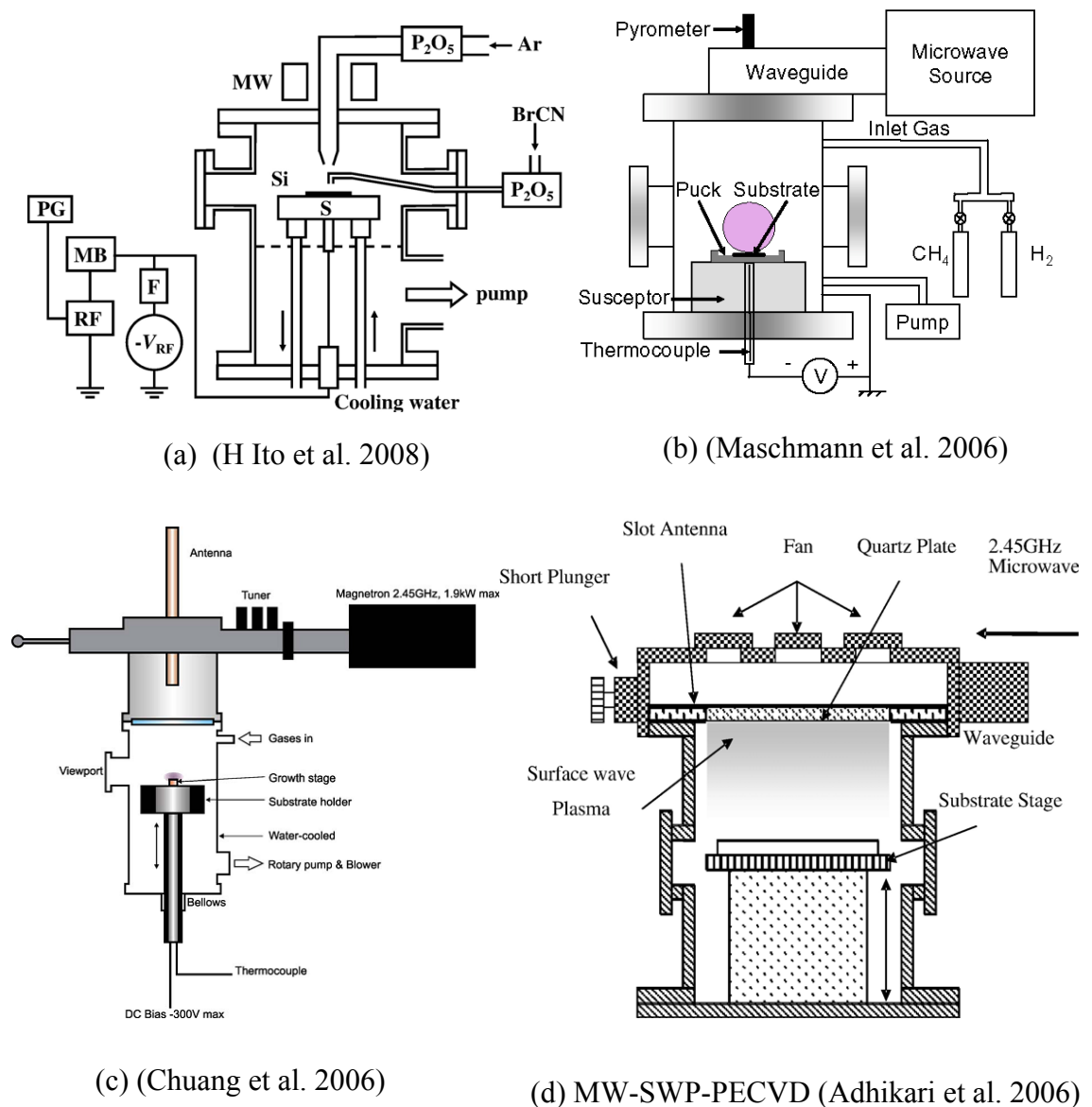


Figure 2.6: Schematic diagrams of various MWCVD systems.

A variation of MWPECVD, namely the microwave surface wave plasma CVD (MW-SWP-CVD) has been developed by Nagatsu et al (Nagatsu et al. 2000; Nagatsu et al. 2002) to produce carbon films without ion bombardment on the substrate. This method greatly reduces the effect of the ion and plasma induced damage on the films and substrates (Ghimire et al. 2006). It has been viewed as one of the most promising plasma sources for large area thin film deposition (Rusop et al. 2005; Rusop et al. 2006) which makes it a prospective mass-production technique particularly for diamond and DLC films (Ghimire et al. 2008).

Variation in the formation of CN_x films using these MWPECVD systems include amorphous CN_x (Ito et al. 2008; Kumar et al. 2010; Omer et al. 2005), nitrogen doped diamond films (Achard et al. 2007; Secroun et al. 2007; Tang et al. 2010) and nanotubes (Brown et al. 2011; Fang et al. 2007; Srivastava et al. 2006). The systems have been shown not only to be able to produce high quality diamond films for hard coating (Tang et al. 2010) but also some which show good photovoltaic properties (Secroun et al. 2007).

2.2.3.4 Electron cyclotron chemical vapour deposition

The setup of a typical electron cyclotron resonance ECR-CVD is similar to that of MEPECVD. The main differences are the magnets placed at specific locations outside the chamber to produce a static magnetic field and the use of an ECR ion source. By superimposing the static magnetic field and high-field electromagnetic field (typically produced by a microwave source) at the ERC frequency, the gas precursors in

the chamber could be excited to form ionized plasma. This plasma drives the formation of the films. Examples of two different setups are shown in Figure 2.7.

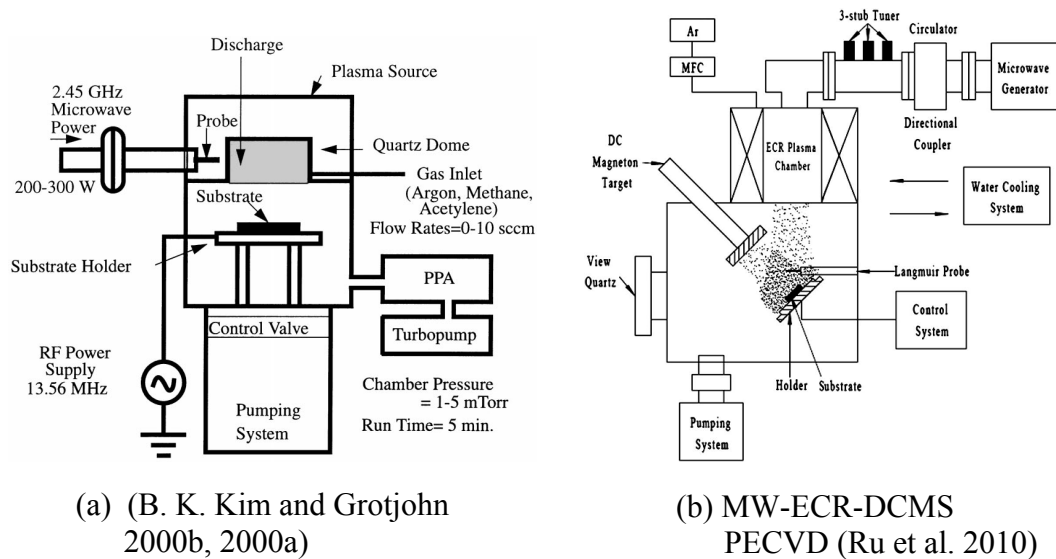


Figure 2.7: Schematic diagrams of different variations of ECRCVD systems.

The ECR plasma, commonly created using microwave power, creates high density ion species (typically 10^{11} - 10^{12} cm^{-3}) at low pressure ranging from sub-millitorr to a few millitorr. This combination of high ion density with a low pressure results in a low neutral density and produces fluxes having a high ion/neutral ratio of species impinging the substrate (Kim and Grotjohn 2000b). This allows a wide range of different film properties to be produced and also reduces hydrocarbon contaminants (Chan et al. 1999), which is one of the main advantages in the ECRCVD method (Lai et al. 2003; Ling et al. 2002; Sung et al. 1999; Wu et al. 2000). The presence of highly energetic electrons created at resonance also results in the creation of hydrocarbon ion species that normally may not be present in conventional plasma CVD (Yoon et al. 1999). A number of researchers have also demonstrated that ECRCVD exhibits an enhancement in the dissociation of dopant precursors such as nitrogen, resulting in increased reactivity within the plasma (Cameron 2003; Chan et al. 1999) and

consequently, in the bond formation with carbon. This would increase the incorporation of the dopant forming various films with different properties.

Further enchantment in the ECRCVD technique includes substrate biasing where dc and rf biases have been used (Kim and Grotjohn 2000b). This biasing influences the energy of the ion flux impinging the substrate. Thus the ECR plasma and substrate biasing allows the ion density and ion energy to be independently controlled (Kim and Grotjohn 2000b; Liu et al. 2001b). Recently there are also numerous modifications of ECRCVD techniques employing both physical and chemical (ECR) methods. Examples of these systems include MW-ECR plasma-enhanced direct current magnetron sputtering (Ru et al. 2010) and ECR plasma-assisted (reactive) pulsed laser deposition (Dong et al. 2008; Ling et al. 2002; Shen et al. 2006). These systems have been implemented in the studies of dopant incorporation for the enhancement of carbon films.

Although ECR CVD appears versatile in the aspect of producing various carbon films, there are relatively few studies pertaining to the formation of CN_x films by this method. Most work focuses on amorphous CN_x films (Camero et al. 2003; Dong et al. 2008; Liu et al. 2001b; Shen et al. 2006), although there are some reports on the formation of hydrogenated amorphous CN_x nanotips (Liu et al. 2000; Omer et al. 2005) and nanorods (Liu et al. 2002).

2.2.3.5 Radio frequency plasma enhanced chemical vapour deposition

Radio frequency, rf-PECVD may well be the simplest system among these PECVDs with advantages of having the capability of homogeneous deposition over a

large substrate area (Wang et al. 2008a), which permits reasonably high deposition rate, good film adhesion, produces films with low pinhole density (Kim et al. 2010) and enables relatively low temperature deposition (Chu and Shiue 2008 ; Le Poche et al. 2007; Qi et al. 2009). In a typical rf PECVD system, a radio frequency generator operating at 13.56 MHz, is used to generate the plasma inside the deposition chamber. The film would form on the substrate which is exposed to the plasma. In most cases a conventional rf generator working at a frequency of 13.56 MHz is employed in rf PECVD. There are two main variations in the system setup which are shown in the examples in Figure 2.8.

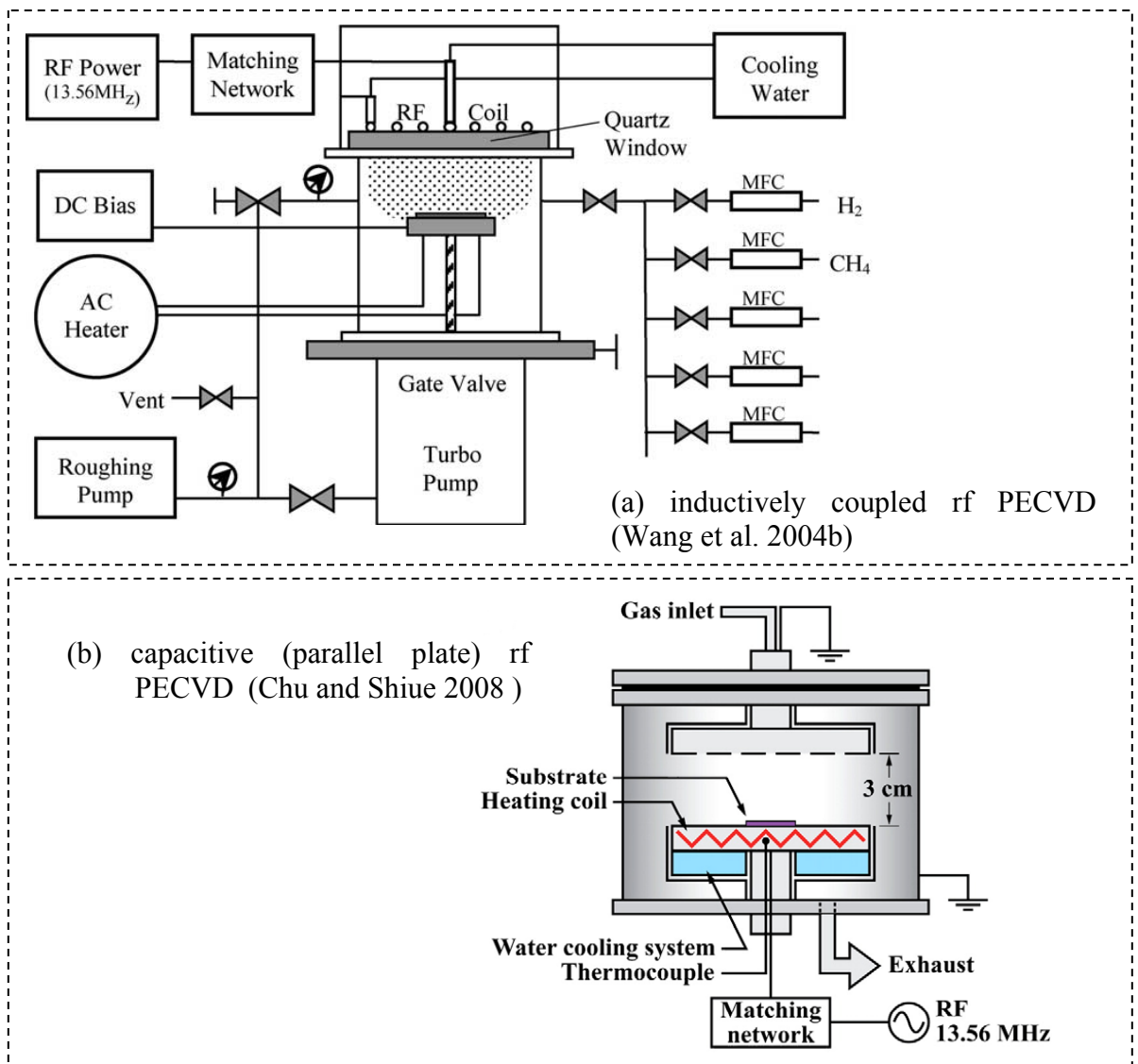


Figure 2.8: Schematic diagrams of two different variations of rf PECVD systems.

In the first setup shown in Figure 2.8(a), the rf energy is inductively coupled into the deposition chamber with a planar-coiled rf antenna normally placed on the outside of a quartz window. The placement of the antenna, being on the outside of the chamber which thus isolates it from the plasma and reduces contamination which otherwise could originate from the ion bombardment of the coil (Wang et al. 2004b; Zhu et al. 2007). The second setup shown in Figure 2.8(b), employs a parallel-plate electrodes configuration, whereby either one of the electrodes is rf powered while the other is either grounded or biased. This is the preferred configuration among these two setups (Smith et al. 2001) and is said to maximize the energetic ion flux at the substrate during the film growth process (Motta and Pereyra 2004). Popular modifications of rf PECVD include the so-called dual dc-rf PECVD which employs a dc bias that allows the flexibility to qualitatively control the ion current density and the ion kinetic energy by adjusting the rf power and dc bias, respectively (Ding et al. 2008; Hao et al. 2005; Hao et al. 2007; Li et al. 2003a). This setup has been used to successfully produce vertically aligned CNTs.

rf PECVD has been proven to be able to produce a wide variety of hydrogenated and hydrogen-free carbon and doped-carbon films. These includes amorphous carbon (Itoh and Mutsukura 2004; Kim et al. 2010; Motta and Pereyra 2004; Mutsukura and Daigo 2003), DLC (Dorner-Reisel et al. 2005; Ohtsu et al. 2007; Shimada et al. 1993; Smietana et al. ; Tzeng et al.) and polymeric (Daigo and Mutsukura 2004; Ghodselahi and Vesaghi 2008) thin films. This method also produces a variety of nanostructured carbon-based films such as carbon nanofibers (Le Poche et al. 2007; Melechko et al. 2005), nanosheets (Liu et al. 2011; Wang et al. 2004b; Zhu et al. 2007; Zhu et al. 2011), nanowalls (Malesevic et al. 2007), nanotubes (Jiang et al. 2006; Liu et al. 2007; Yabe et al. 2004) and graphene (Liu et al. 2011; Somani et al. 2006; Wang et al. 2004a). Indeed,

rf PECVD could produce almost all known structures of carbon films. DLC films are normally obtained at high deposition (substrate) temperatures at high hydrogen-to-methane ($H_2:CH_4$) gas flow-rate ratios. In contrast, low deposition temperatures or/and the used of dopant gas dilution normally yield polymeric films. On the other hand, nanostructures such as nanotubes and nanofibers are typically obtained with the assistance of metal catalysis or templates at moderate temperatures (above 450 °C). Nanosheets, nanowalls and graphene could be obtained without metal catalysis, though the deposition temperature requirements are higher (typically above 600 °C).

Recent studies have reported the use of rf PECVD in the formation of various CN_x films. This include hydrogenated amorphous films (Kim et al. 2010; Kumar et al. 2010), polymer-like (Pereira et al. 2005), diamond-like (Dorner-Reisel et al. 2005), fullerene-like (Gago et al. 2005), CN_x particles (Pereira et al. 2005) and nitrogen doped CNTs (Noh et al. 2010). Through the use of this technique Kim et al. (Kim et al. 2010) report enhanced hardness and optical transparency in a- CN_x as compared to a-C, making it suitable as a hard mask for nanopatterning. Similarly, the system could deposit CN_x films which shows enhancement in numerous applications such as hard coatings (Itoh and Mutsukura 2004), photovoltaic devices (Chu and Shiue 2008), water repellent coatings (Lin et al. 2007) and optoelectronics (Daigo and Mutsukura 2004).

2.3 Choice of Deposition Technique

The choice of deposition method employed in this study was governed by two main factors. Firstly, since this system was a home-built system it was important to choose a system that is not only relatively cheap to build but is also easy to design and

operate. Furthermore this system should be able to be modified easily and should yield good quality homogeneous films. The final reason (which is the most important) is that the system must be versatile and be able to produce a variety of CN_x structures. It was also important to be able to use this system for future work as a continuation of this study.

Among the deposition systems studied, rf PECVD seems the best choice. This system is relatively simple as compared to MW and ECR PECVD. rf PECVD is not only easy to design, cost less to assemble and maintain, but is simpler to handle and modified accordingly. Although this system is relatively more complex than TCVD and HFCVD, rf PECVD can operate at much lower temperature to produce vertically aligned nanostructured films. Furthermore, TCVD and HFCVD would nearly always require catalytic assistance and extremely high deposition temperatures to produce their fibrous nanostructured films. It is of great interest to determine if this versatile rf PECVD method could form these fibrous nanostructured films without metal catalysis and at low temperatures.

2.4 Review on Analytical Methods

In this section, some important literature reviews on the interpretation of the characterization tools used in this work is presented. Excluded from this section are theories on surface profilometer, field effect scanning electron spectroscopy (FESEM), high resolution transmission electron microscopy (HRTEM) and Auger electron spectroscopy (AES). These measurements allow direct analysis or calculations to be extracted either from the images obtained (FESEM and HRTEM) or using the relevant

software available, such as in the composition calculations for AES. Instead, this section presents reviews of the optical properties, Raman scattering spectroscopy, Fourier transform infrared spectroscopy and photoluminescence. These are employed in the characterization of the CN_x films presented in chapter 4, 5 and 6.

2.4.1 Optical properties

The optical energy gap for CN_x films is closely related to their relative sp^1 , sp^2 and sp^3 content and the presence of disorder in the films. The cluster model is commonly employed in the explanation of the gap in carbon films depicts graphite-like or polyaromatic islands with sp^2 bonding embedded in hydrogenated tetrahedrally bonded sp^3 matrix (Ferrari and Robertson 2000; Gharbi et al. 2008). A thorough study of the relationship between the optical energy gap and this model has been discussed by Robertson (Robertson 1995, 1997, 2002a; 2002b; 2003). A brief summary of the reports are discussed below.

The sp^3 sites, which control the mechanical properties of these films, form four σ bonds, while sp^2 sites form three σ bonds and a weaker π -bond. The σ bonds of these sp^2 and sp^3 sites generate σ valence and σ^* conduction band states. These states are said to be separated by a wide band gap of ~ 6 eV (Robertson 1997). The π -bond in the sp^2 sites creates π valence and π^* conduction states within the σ - σ^* gap. By perturbation theory, these states control the details of the structure since they lie closest to the Fermi level (Robertson 2002b). They also form the localized band edges and determine the optical energy gap. To maximize the bonding energy and stability, the π -bonds would attempt to pair up, and may

even form six-fold planar aromatic rings. Further stabilization would see the formation and growth of graphitic clusters, made up of these fused aromatic rings. These clusters form islands segregated in the sp^3 matrix, giving the proposed cluster model. The resulting optical energy gap would depend on the size and distribution of these clusters where the width of the band gap varies inversely with the sp^2 cluster size.

Recent studies on the optical properties of CN_x films support this theory. Alibert et al. (Alibert et al. 2008a) showed that the optical (and optoelectronic) properties of their sputtered CN_x films depend not only on the N content but also on microstructure versus N content, which is related to their relative sp^1 , sp^2 and sp^3 contents. The connectivity of the sp^2 clustering and organization significantly influence the optical gap. In another study done by Alibert et al. (Alibert et al. 2011), it was seen that the increase in nitrogen incorporation induces the formation of $C\equiv N$ terminating bonds which affects this connectivity, and therefore, the sp^2 cluster size and their relative disorder. Here there appears to be a critical N content where the optical energy gap begins to increase. In contrast, other researchers have reported a general decrease in optical energy gap with increasing N content (Adhikari et al. 2008; Meškinis et al. 2010; Ralchenko et al. 2007). This was due to the increase in sp^2 bonds and resulting cluster size in the CN_x film with the increase in N incorporation. Such contrasting results further emphasize the importance of determining the bonding properties of the CN_x films in this study.

2.4.2 Raman spectroscopic studies on carbon nitride thin films

Raman spectra of carbon films are strongly dependent on their structure, whether they are diamond, graphite, amorphous, nanocrystalline, etc. These spectra tend to show specific trends which could be used to identify the structure of the films. Some examples of these spectra with reference to those discussed by Chu and Li (Chu and Li 2006), are shown in Figure 2.9.

The Raman spectra for carbon nitride are the same as those of nitrogen-free amorphous carbon which have the same structure. (Chen et al. 1993; Ferrari and Robertson 2000; Ferrari et al. 2003b). Two variants in the peaks normally assigned as G and D peaks are discussed in relation to the sp^2 components in the material. The G peak, usually found at approximately 1575 cm^{-1} reflects the zone-centred E_{2g} mode of graphite peak and is due to all pairs of sp^2 atoms in both rings and chains. The D peak at 1355 cm^{-1} which is due to the breathing modes of A_{1g} symmetry involves phonons near the K zone boundary and is attributed to sp^2 sites only in aromatic rings (Lin et al. 2007) and only becomes active in the presence of disorder. The Raman characteristics are said to depend on four main aspects which includes (Ferrari and Robertson 2000):

- 1) clustering of the sp^2 phase
- 2) bond disorder
- 3) presence of sp^2 rings or chains
- 4) sp^2/sp^3 ratio

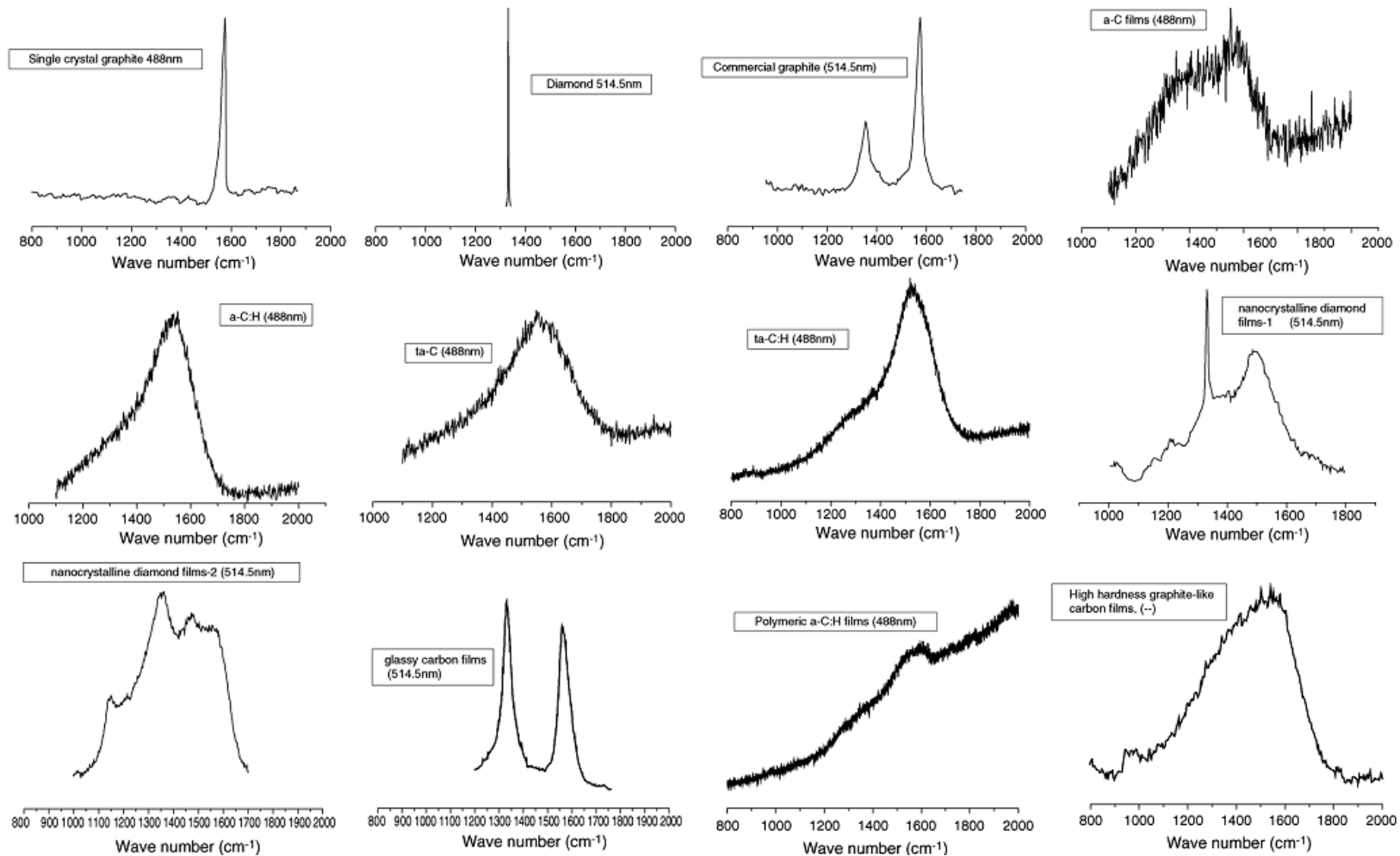


Figure 2.9: Examples of typical Raman spectra for different carbon film structure at different excitation wavelength. Figures are taken from those illustrated by Chu and Li (Chu and Li 2006)

One of the simplest methods in the interpretation of the Raman D and G peak assessment is through the peak deconvolution using Gaussian fittings. From the integrated peaks, five parameters are calculated which includes the band-position (ω) and bandwidth of both G and D bands and the ratio of the integrated intensities of D band to G band, I_D/I_G . The width is calculated as the full width half maximum (FWHM) of the fitted peaks.

I_D/I_G enables assessment of the degree of disorder (Chu and Li 2006), the evolution clusters in the films (Ferrari and Robertson 2000) and its distribution (Cheng et al. 2001b). For ordered materials such as graphite, I_D/I_G will increase with the increase in disorder (Ferrari and Robertson 2000; Freire et al. 1995) since the presence of the D band is an indication of disorder in the material (Freire et al. 1995). However, for disordered materials such as a-C, the presence of the D peak may indicate ordering since the D band originates from the presence of six-fold rings and its intensity is proportional to the probability of finding the six-fold ring in the cluster (Ferrari and Robertson 2000). In such amorphous materials, the variation in I_D/I_G is also dependent in the number and/or size of these clusters (Cheng et al. 2001b; Dillon et al. 1984; Lacerda et al. 1998; Lee and Kang 2001).

The interpretation the I_D/I_G ratio is normally accompanied by the assessment of the G band. The polymeric nature of the films deposited in this work, determined from its high PL background, fits these films in Stage 2 of the amorphization trajectories proposed by Ferrari and Robertson (Ferrari and Robertson 2000, 2001; Ferrari et al. 2003b, 2003a). C or CN_x films of Stage 2 are sp^2 -dominated, consisting of nanometer sized two-dimensional clusters. The G peak can either be red-shifted (to lower wavenumber) or blue-shifted (to higher wavenumber) compared to the 1580 cm^{-1} G

position of graphite. Red shift occurs due to an increase in non six-fold rings in the sp^2 -clusters. The G peak is blue-shifted only for glassy carbon-like structures with a dominantly graphene-like ordering. In such a case the G peak's Raman shift can reach 1600 cm^{-1} . Also since the G band is associated with all pairs of sp^2 atoms in both rings and chains, the red-shift in its position (and also the D band position), reflects a larger degree of bond angle or bond length disorder (Shiao and Hoffman 1996). Conversely, the decrease (narrowing) in the G bandwidth indicates the removal of bond angle and bond length disorder (Chu and Li 2006; Knight and White 1989; Shiao and Hoffman 1996) thus implying an increase in ordering.

The blue shift of the D peak position is due to small size aromatic clusters consisting of only six-fold rings (Ferrari and Robertson 2000; Kovács et al. 2008). This blue shift is also an indication of the increase in disorder (Ferrari and Robertson 2000). Two contributing factors may cause the red shift in the D peak position. The first is a decrease in the number of ordered aromatic rings (Ferrari and Robertson 2000, 2001; Ferrari et al. 2003b), while the second can be attributed to strained or curved graphite plane, which may lead to a change in the space between the atoms (Yu et al. 2002c). The broadening of the width of the D peak is correlated to the increase in disorder due to a distribution of clusters with different orders and dimensions (Ferrari and Robertson 2000). Similarly, the decrease in width of the D peaks (and G peak) may correspond to the increase in ordering due to the removal of bond-angle disorder and increase in dominance of crystallites (Yu et al. 2002c).

Raman scattering allows excellent prediction of the structure of the CN_x films. The Raman analyses of works carried out by Wang et al. (Wang et al. 2008a, 2008b) indicate that N incorporation favours the formation of sp^2 units and that the presence of

the D band in the amorphous carbon is an indication that the sp^2 are in the form of aromatic rings. They have suggested that the N content in CN_x films would induce either an increase in order implied by an increase in I_D/I_G , or an increase in disorder with the decrease in I_D/I_G . Panchakarla et al. (Panchakarla et al. 2010) have suggested that the disorder-induced D band is particularly sensitive to doping, especially for ordered structures such as CNTs. In the investigation of N incorporation of DLCs, Tang et al. (Tang et al. 2010) showed that the increase in the width of the D band with the increase in N incorporation indicates a degradation in these DLC quality.

Other researchers have also used Raman scattering characteristics to identify and quantify a number of different structured CN_x films. They have studied various N doped carbon films, consisting of amorphous CN_x (Ghimire et al. 2008; Kim et al. 2010), DLC (Nakazawa et al. 2010; Ralchenko et al. 2007), nanocolumn and nanoporous CN_x (Zhang et al. 2010a), CNTs (Liu et al. 2010; Xu et al. 2010) and graphenes (Imran Jafri et al. 2010; Wang et al. 2011a).

2.4.3 *Fourier transform infrared spectroscopy*

Fourier transform infrared (FTIR) spectroscopy is without doubt one of the most common tools in the characterization of CN_x films, whether they are in the form of thin or as nanostructured films. Although IR radiation constitutes a broad electromagnetic spectrum range between visible and microwave regions, it is the limited wavenumber portions from 4000 to 400 cm^{-1} that is of greatest practical use. Within this region a number of vibrational modes can be detected and assigned to various bonds in the films. These bonds are related to specific groups of atoms which give rise to distinct energy

levels at or near the same frequency regardless of the structure of the films. The variation in vibrational modes is shown in Figure 2.10.

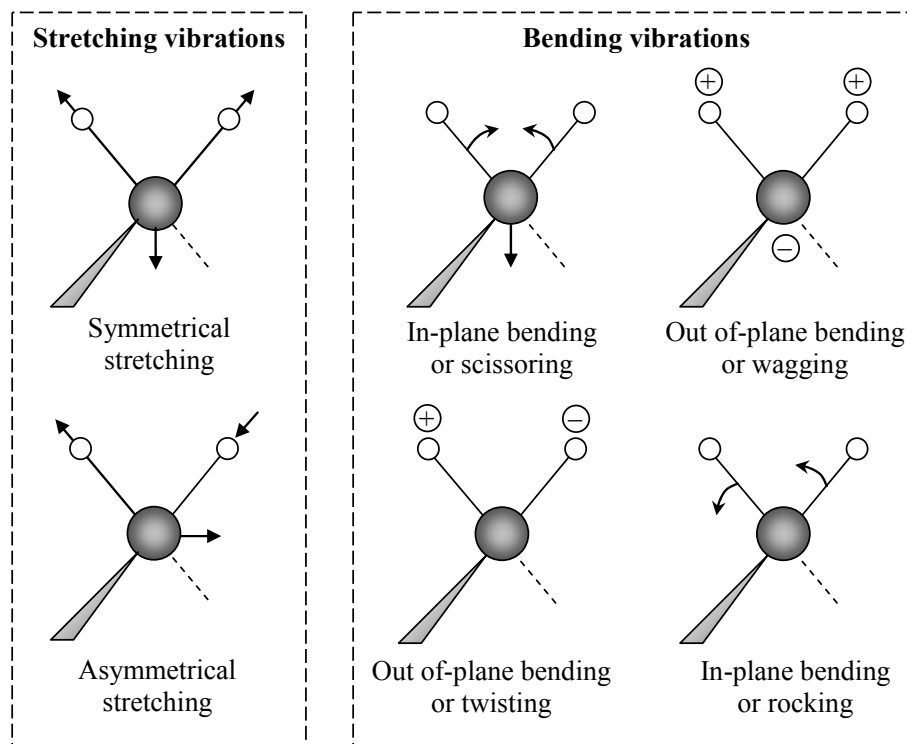


Figure 2.10: Vibration modes for CH_2 group. (+ and – indicate movement perpendicular to the plane of this page) (Silverstein and Webster 1997)

The assessment of the FTIR spectra requires accurate quantitative determination of the peak intensities and positions. This is often difficult since the bonds tend to have energy values that are close together, such that the corresponding peaks would overlap and form broad band regions instead of clear sharp peaks. A popular method of solving this is by carrying out deconvolution of these broad peaks using Gaussian fittings. A typical FTIR spectrum for CN_x film obtained in this work is shown in Figure 2.11 which shows three distinct regions of interest pertaining to different bonding characteristics of the films.

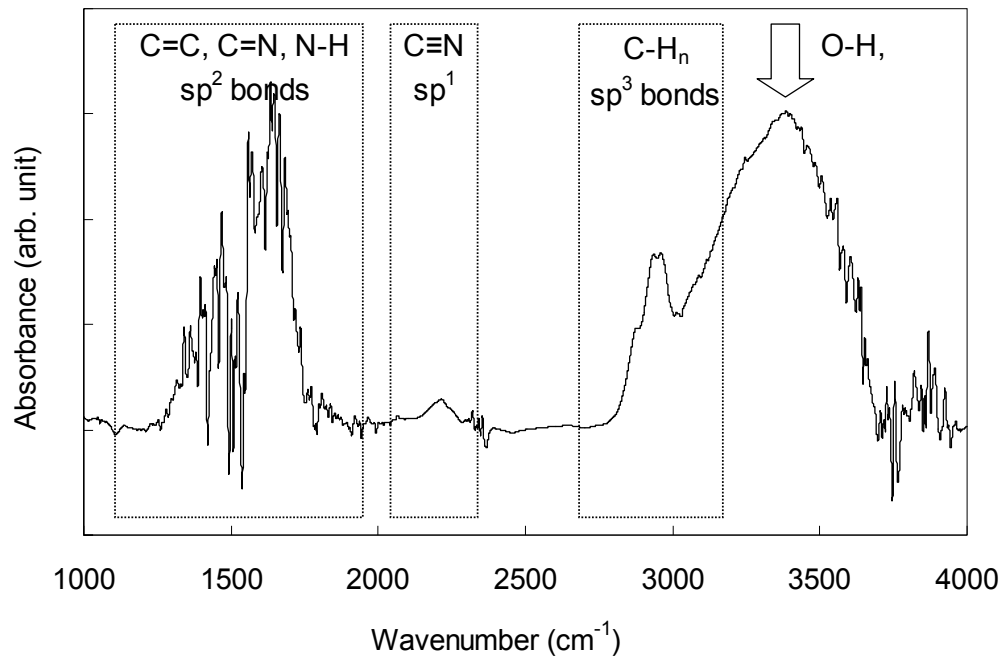


Figure 2.11: Example of typical Fourier transform infrared spectrum for carbon nitride films obtained in this work.

The spectra were deconvoluted within each regions according to the fitting method proposed by some researchers (Fanchini et al. 2005; Ghodselahi and Vesaghi 2008; Gottardi et al. 2008; Lazar et al. 2005). The list of functional groups adopted in this work is listed in Table 2.1. Note that these assignments are taken from references which assess the bonds within each region as a whole to attain the sets of bonds as shown in the list. Individual assignment of the bonds could be referred from the references within the list.

Table 2.1: List of bonding assignments, wavenumber regions and corresponding references.

Range (cm ⁻¹)	Assignment	Wavenumber (cm ⁻¹)	Reference
1000 – 1800	C=C, C=N, N-H	1620-1650	(Chu and Li 2006; Lazar et al. 2005; Motta and Pereyra 2004)
	Raman G band	1550-1570	
	sp ³ CH _x	1450	
	Raman D band	1360-1380	
	sp ² C, C-N, C=N	1300-1350	
	C-N	1220-1265	
2000 – 2300	[C ₂ H] _n -C≡N	2245	(Kundoo et al. 2003; Mutsukura and Akita 2000; Mutsukura 2001; Mutsukura and Daigo 2003)
	aromatic [C ₆ H ₆]-C≡N	2215	
	[CH ₃]-N≡C	2190	
	C ₂ H ₅ -N≡C	2160	
	aromatic [C ₆ H ₆]-N≡C	2105	
	HCN	2060	
2700 – 3800	sp ² CH ₂	3020	(Fanchini et al. 2005; Ghodselahi and Vesaghi 2008; Gottardi et al. 2008; Lazar et al. 2005; Pereira et al. 2005)
	sp ² CH	3000	
	asym sp ³ CH ₃	2960	
	asym sp ³ CH ₂	2930	
	sym sp ³ CH ₃	2875	
	sym sp ³ CH ₂	2835	

2.4.4 Photoluminescence properties of carbon nitride thin films

Investigation of the photoluminescence (PL) characteristics of CN_x films have been of keen interest for both fundamental and practical purposes. They allow the study of the potential of these materials in electroluminescence (EL) devices (Daigo and Mutsukura 2004; Zhang et al. 1999b), the study of electronic states from the features of

the PL spectra (Fanchini and et al. 2002; Panwar et al. 2006) and the mechanism of carrier recombination (Fanchini et al. 2003; Robertson 1997). PL characteristics for carbon based films were found to be more tolerant of defects and could exist at much higher defect densities (Panwar et al. 2006; Robertson 1996a). Their PL efficiency were also found to be independent of temperature and not quenched by electric field (Panwar et al. 2006). These characteristics increase the potential of a-C films as electro-optical devices. Indeed C and CN_x films have been shown to exhibit good EL properties (Daigo and Mutsukura 2004; Zhang et al. 1999b) and even showed bright white EL emission (Kim and Wager 1988).

The PL emission of these films could be enhanced by nitrogen incorporation where the PL intensity depends on the nitrogen content (Zhang et al. 1999b). Although the role of nitrogen remains controversial, their PL characteristics and mechanism are similar to those of carbon films. The most widely accepted model is the geminate recombination of electron-hole pairs within sp² bonded clusters in the sp³ bonded amorphous matrix (Panwar et al. 2006) which mirrors the cluster model. The sp³ bonded regions create a potential barrier which confines the π states of the sp² clusters. This result is the formation of highly localized sites which creates the π tail states and act as radiative recombination centers. Photo carriers can recombine inside the clusters themselves by phonon emission (Gharbi et al. 2008) and this produces PL emission. Thus the cluster size and distribution also affects the PL intensity and efficiency. The PL efficiency corresponds to the integrated PL energy under the condition of a fixed light (laser) source intensity and beam area.

A complication in the assessment of electronic states in these films is that the gap states do not separate simply into tail and defects states but according to

demarcation levels. Only states between the electron and hole demarcation level act as recombination centers, while those above or below may act as traps (Robertson 2003). The loss of PL efficiency occurs due to non-radiative recombination within these traps. This recombination arises from numerous types of defect states in the films. PL is said to be quenched if the defect density exceeds a certain value, since the electron-hole pairs are always formed within a capture radius of a defect (Robertson 1996b, 2003). Figure 2.12 shows a schematic diagram of the proposal by Robertson (Robertson 1997, 2003) for the PL mechanism.

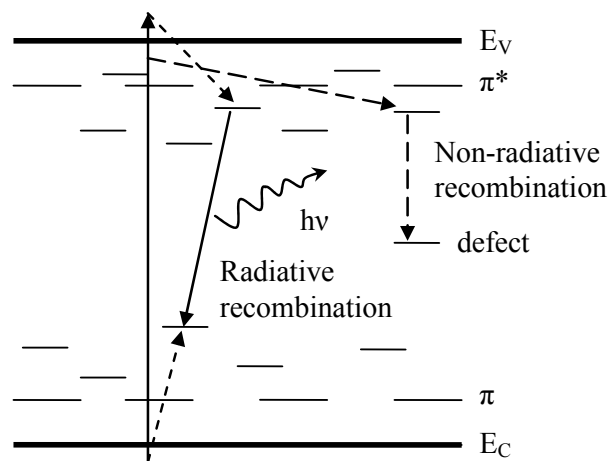


Figure 2.12: Schematic diagram of proposed photoluminescence mechanism (Robertson 1997, 2003).

PL emission for CN_x is normally seen as a broad band. Its mean energy increases at half the rate of the film's optical energy gap (Robertson 2003). The broad spectrum is attributed to a wide energy range of its luminescence centers. This in turn is attributed to the different cluster sizes and shapes in the film (Zhang et al. 1999b). There have been a number of studies done to determine the origin of defect sites and also on the roles of hydrogen and nitrogen incorporation on the PL efficiency. It has been said that dangling bonds which form defect sites may contribute to the PL variation (Gharbi

et al. 2008), though Robertson (Robertson 1997) has suggested that paramagnetic defects may play a more dominant role in reducing PL intensity.

For such materials as amorphous silicon films, hydrogen incorporation would passivate these dangling bonds, thus reducing the defect states. However the role of hydrogen in carbon based films is more complicated. Panwar et al (Panwar et al. 2006) suggested that hydrogen does not passivate these dangling bonds but in general might even cause more problems or instability in the material. Nevertheless, hydrogen does lower the defect density, not by filling up the dangling bonds but by reducing the cluster size and thereby increasing the defect creation energy to reduce their thermodynamic probability (Robertson 1983).

On the other hand nitrogen affects the PL characteristics in a number of different ways. Since the size of nitrogen atoms is comparable to carbon, substitutional sites could be formed in the carbon network. When a nitrogen atom substitute for a sp^3 coordinated carbon atom, the average coordination number reduces which in turn reduces the internal stress and the resulting distortions in the sp^2 clusters (Zhang et al. 1999b). At higher nitrogen content, the formation of compact clusters with N-H, C=N and C \equiv N bonds would be formed. These bonds have been said to influence the PL efficiency of CN_x films (Daigo and Mutsukura 2004; Mutsukura and Akita 2000; Mutsukura 2001). Also, the role of lone-pairs attributed to the sp^1 hybridized sites (C \equiv N) could either enhanced or reduce the PL efficiency. The enhancement could occur if the lone-pair forms weak bonds with the π and π^* states resulting in the mentioned mixed lone-pair/ π states. Since the lone-pairs could also form strong localized states, this would broaden the localized states in the system which act as the radiative recombination centers and thus enhance the confinement of electrons. On the other

hand, if these lone-pairs remain unbonded, they may instead act as non-radiative centers and thus reduce the PL properties (Fanchini et al. 2003).

Apart from these factors, Fanchini et al (Fanchini et al. 2003) have also determined a relationship between the strength (and thus the content) of OH bonds in the film and the PL efficiency. The increase in the OH bonds and thus the porosity of the film, result in an increase in the PL intensity. This is because the OH bonds can either enhance the electron-hole confinement or/and reduce internal stress in the film and thus decrease the number of distorted sites.